arXiv:1606.02742v1 [hep-lat] 8 Jun 2016

A study of symmetry breaking in a relativistic Bose gas using the contraction algorithm

Andrei Alexandru
Department of Physics, George Washington University, Washington, DC 20052 and
Department of Physics, University of Maryland, College Park, MD 20742

Gökçe Başar, Paulo Bedaque, Gregory W. Ridgway, and Neill C. Warrington
Department of Physics, University of Maryland, College Park, MD 20742

(Dated: June 10, 2016)

A relativistic Bose gas at finite density suffers from a sign problem that makes direct numerical simulations not feasible. One possible solution to the sign problem is to re-express the path integral in terms of Lefschetz thimbles. Using this approach we study the relativistic Bose gas both in the symmetric phase (low-density) and the spontaneously broken phase (high-density). In the high-density phase we break explicitly the symmetry and determine the dependence of the order parameter on the breaking. We study the relative contributions of the dominant and sub-dominant thimbles in this phase. We find that the sub-dominant thimble only contributes substantially when the explicit symmetry breaking is small, a regime that is dominated by finite volume effects. In the regime relevant for the thermodynamic limit, this contribution is negligible.

I. INTRODUCTION

The Monte Carlo method is a powerful tool to study field theories even when perturbation theory and other analytical methods fail. The method is usually applied in the Euclidean time formalism where the path integral defining the field theory becomes equivalent to a statistical mechanics problem: each field configuration is sampled according to a Boltzmann factor $\exp(-S)$, with S being the Euclidean action for the configuration, and the observables are expressed as correlations of composite field operators. The Monte Carlo method, however, has its limitations. When the action is not real, as is often the case in the presence of a chemical potential, this approach fails. A possible solution is to use the real part of the action S_R for importance sampling and combine the imaginary part with the observable, that is, to replace $\mathcal{O}$ with $\mathcal{O}\exp(-iS_I)$. For theories that exhibit the *sign problem*, the phase factor fluctuates substantially and the signal-to-noise ratio for $\langle\exp(-iS_I)\rangle$ decreases exponentially fast as the volume increases. This renders the stochastic approach unfeasible.

Recently it was suggested that the sign problem can be solved by re-expressing the path integral using Lefschetz thimbles [1]. The idea is to take the original path-integral expressed in terms of n real degrees of freedom and view it as an integral over the $\mathbb{R}^n$ submanifold embedded in $\mathbb{C}^n$. Smooth deformations of the integration domain will not change the value of the integral as long as we do not cross any singularities of the integrand and we keep the integral finite. While the integral remains the same, the fluctuations of the integrand on some of these manifolds could be reduced, making this formulation better suited for numerical sampling. A particular choice, and in a certain sense the optimal one, is the decomposition of the original integration domain in terms of Lefschetz thimbles, manifolds that have constant S_I [1]. If the decomposition involves only one thimble, or if one thimble dominates the path integral, then the sign problem is solved. This does not seem to be the case for theories in $0+1$ dimensions, even in the continuum limit [2–4], but there is still a hope that this might happen in the thermodynamic limit or in the continuum limit for quantum field theories [1]. We note that even if this is not the case, there is a possibility that alternative methods based on other manifolds might be numerically useful [5].

In this paper we study the relativistic Bose gas at finite density using the contraction algorithm. This system has a complex action leading to a sign problem. In the last few years this system was used as a test case for different approaches to the sign problem: complex Langevin [6], dual variables [7, 8], mean field [9, 10], density of states [11], and Lefschetz thimbles [12, 13]. Our goal is to understand the interplay between spontaneous symmetry breaking and the contribution of non-dominant thimbles, to showcase the contraction algorithm [2] and some of the optimizations we developed [14], and to test some ideas about using alternative manifolds as integration domains [5]. In a recent study it was conjectured that the tangent space at the critical point of the dominant thimble is equivalent with the integration over the original domain [12]. We confirm this conjecture numerically by showing that the results of our algorithm match very well the results from alternative approaches. Using this result as a benchmark we check the relative contribution of the dominant thimble.

The plan of the paper is the following. In Section II we review the relevant details about the thimbles and describe the algorithm we used to perform the integral over the thimble(s). In Section III we introduce the action for the relativistic Bose gas, its discretization and discuss the details relevant for our implementation. In Section IV we present the results of our method and compare it with results from other approaches. In Section V we draw conclusions and discuss future directions.

II. LEFSCHETZ THIMBLES AND THE CONTRACTION ALGORITHM

Thermal expectation values of observables in a bosonic field theory have the path integral expression

$$\langle \mathcal{O} \rangle = \frac{1}{Z} \int D\phi \, e^{-S(\phi)} \mathcal{O}(\phi) \quad \text{with} \quad Z = \int D\phi \, e^{-S(\phi)}, \tag{2.1}$$

where the integration is taken over real fields ϕ, and S is the Euclidean action. In practice, to compute the path integral above, one first regulates the theory by approximating spacetime by a lattice of points. The effect of this regularization on the path integral is to change the integration domain from the space of field configurations to $\mathbb{R}^n$, where n is the number of degrees of freedom. When S is real, the observables can be evaluated by a Monte Carlo integration, that is, $\langle \mathcal{O} \rangle$ is estimated as

$$\langle \mathcal{O} \rangle \approx \frac{1}{\mathcal{N}} \sum_{a=1}^{\mathcal{N}} \mathcal{O}(\phi_a), \tag{2.2}$$

where the field configurations ϕ_a are distributed according to the probability distribution $\Pr(\phi) = \exp[-S(\phi)]/Z$. The Monte Carlo method does not work when the action $S = S_R + iS_I$ is complex. A possible solution to this problem is the so-called "reweighting" procedure which amounts re-expressing the original observable as a ratio of observables, which is amenable to a standard Monte Carlo evaluation:

$$\begin{aligned} \langle \mathcal{O} \rangle &= \frac{1}{Z} \int D\phi \, e^{-(S_R + iS_I)} \mathcal{O} \\ &= \frac{1}{Z/Z_R} \frac{1}{Z_R} \int D\phi \, e^{-S_R} \left(\mathrm{e}^{-iS_I} \mathcal{O} \right) = \frac{\left\langle e^{-iS_I} \mathcal{O} \right\rangle_{S_R}}{\left\langle e^{-iS_I} \right\rangle_{S_R}} \end{aligned} \tag{2.3}$$

where $\langle \cdot \rangle_{S_R}$ denotes an average with respect to the probability distribution $\exp(-S_R)/Z_R$ with $Z_R = \int D\phi \, \exp[-S_R(\phi)]$. Unfortunately the denominator in the equation above scales as $\exp(-\beta V \Delta f)$, where β is the inverse temperature, V is spatial volume, and Δf is the free energy difference between the system described by actions S_R and S. Consequently, the denominator goes to zero exponentially fast as the lattice volumes increases, and any reweighted Monte Carlo is dominated by statistical errors.

An elegant, geometric solution to the sign problem was recently proposed in [1]. The strategy is to first complexify the field variables ϕ, then deform the integration domain from $\mathbb{R}^n$ to another submanifold of $\mathbb{C}^n$. A particularly judicious choice of submanifold is a set of "Lefschetz thimbles", which we will denote by $\{\mathcal{T}_\sigma | \sigma = 1, 2 ...\}$. We first define thimbles, then explain their utility in solving the sign problem. For every critical point ϕ_c of the action, defined by

$$\left. \frac{\partial S}{\partial \phi} \right|_{\phi_c} = 0 \,, \tag{2.4}$$

there is an associated thimble. The thimble $\mathcal{T}$ is defined as the set of all points that, when evolved using the *downward flow equations*

$$\frac{d\phi_i}{dt} = -\overline{\frac{\partial S}{\partial \phi_i}}, \tag{2.5}$$

converge to ϕ_c as $t \to \infty$. An analogous *upward flow* is defined by flipping the sign on the RHS of Eq. 2.5 and an unstable thimble $\mathcal{K}$ can be defined with respect to this flow. Denoting the complexified field variables $\phi_i = \phi_{R,i} + i\phi_{I,i}$, decomposing the effect of the downward flow on its real and imaginary parts and utilizing the Cauchy-Riemann conditions, it can be seen that any trajectory along the downward flow follows a negative gradient flow of with respect to S_R and a Hamiltonian flow with respect to S_I:

$$\begin{aligned} \frac{d\phi_{R,i}}{dt} &= -\frac{\partial S_R}{\partial \phi_{R,i}} = \frac{\partial S_I}{\partial \phi_{I,i}} \,, \\ \frac{d\phi_{I,i}}{dt} &= -\frac{\partial S_R}{\partial \phi_{I,i}} = -\frac{\partial S_I}{\partial \phi_{R,i}} \,. \end{aligned} \tag{2.6}$$

The decomposition above shows that thimbles are the multi-dimensional generalization of steepest descent/stationary phase paths from asymptotic analysis. The imaginary part of the action is then constant over a thimble and it is thus advantageous to deform the region of integration from $\mathbb{R}^n$ to thimbles if there is a rapidly oscillating phase in the integral on $\mathbb{R}^n$. This procedure solves the sign problem. Typically, there are many critical points, and hence many thimbles. Moreover it is a non-trivial task to determine what combination of thimbles is equivalent to the original domain of integration $\mathbb{R}^n$. However, a fundamental result of Picard-Lefschetz theory shows that any integral over $\mathbb{R}^n$ can be decomposed into integrals over thimbles [15, 16]:

$$\int_{\mathbb{R}^n} d\phi \, e^{-S(\phi)} \mathcal{O}(\phi) = \sum_\sigma n_\sigma e^{-iS_I(\phi_\sigma)} \int_{\mathcal{T}_\sigma} d\phi \, e^{-S_R(\phi)} \mathcal{O}(\phi) \,, \tag{2.7}$$

where the summation runs over the critical points ϕ_σ and $\mathcal{T}_\sigma$ are the associated thimbles. The integers n_σ count the intersection points between the original integration contour $\mathbb{R}^n$ and the unstable thimble $\mathcal{K}_\sigma$. The n_σ can be negative: if the flow takes a volume element around one of these intersection points in $\mathbb{R}^n$ into a thimble volume element with orientation opposite to that of the thimble, then the intersection point counts negatively toward n_σ. Therefore, n_σ is the number of points that flow from $\mathbb{R}^n$ to the critical point ϕ_σ via the upward flow while preserving orientation, minus the number of intersection points that reverse orientation.

It is in general very difficult to find all critical points and the values of the coefficients n_σ in the thimble decomposition above. However, assuming none of the n_σ are zero, we see from Eq. 2.7 that we can estimate the relative importance of each thimble based on the value of the real part of the action at the critical point, $S_R(\phi_\sigma)$. The critical point with the lowest action, $\phi_{\bar{\sigma}}$, is expected to

give the largest contribution to the path integral while the subdominant ones are suppressed by a factor $\exp(-\Delta S)$ with $\Delta S = S_R(\phi_\sigma) - S_R(\phi_{\bar\sigma})$. This estimate, of course, neglects entropy effects and it is valid only to the extent that the semiclassical expansion is qualitatively correct. When the main thimble dominates the integral averages can be approximated by

$$\langle \mathcal{O} \rangle \approx \int_{\mathcal{T}_{\bar\sigma}} d\phi\, e^{-S_R(\phi)} \mathcal{O}(\phi) \Big/ \int_{\mathcal{T}_{\bar\sigma}} d\phi\, e^{-S_R(\phi)} \,. \tag{2.8}$$

Notice that the phase fluctuations are almost absent in this case since the imaginary part of the action factors out for observable averages and the sampling is done using the real part of the action. The only remaining phase is the *residual phase*, that is the phase associated with the volume element $d\phi/|d\phi|$, which in general varies smoothly over the thimbles and can be easily reweighted [2, 13, 17].

One of the goals of this paper is to apply the "contraction algorithm" [2, 5] for a relativistic bose gas at finite density. We briefly review the algorithm here. A basic ingredient is the map generated by the upward flow $\phi_n \to \phi_f(\phi_n)$

$$\frac{d\phi}{dt} = +\overline{\frac{\partial S}{\partial \phi}} \quad \text{with} \quad \phi(0) = \phi_n \quad \text{and} \quad \phi_f = \phi(T_{\text{flow}}) \,. \tag{2.9}$$

This is a map from $\mathbb{C}^n$ to $\mathbb{C}^n$. Under this map the value of S_R at every point increases while S_I remains fixed. For any integration manifold $\mathcal{M}_n$ with a finite integral $\int_{\mathcal{M}_n} d\phi\, \exp[-S(\phi)]$, it can be shown that the value of the integral is unchanged if we replace the manifold $\mathcal{M}_n$ with its image through this map, $\mathcal{M}_f = \phi_f(\mathcal{M}_n)$ [5]. Take for the moment $\mathcal{M}_n$ to be the original integration contour $\mathbb{R}^n$. We have

$$\begin{aligned} \int_{\mathbb{R}^n} d\phi\, e^{-S(\phi)} &= \int_{\mathcal{M}_f} d\phi_f\, e^{-S(\phi_f)} \\ &= \int_{\mathbb{R}^n} d\phi_n\, \det J e^{-S(\phi_f(\phi_n))} \quad \text{with} \quad J_{ij} = \frac{\partial (\phi_f)_i}{\partial (\phi_n)_j} \,. \end{aligned} \tag{2.10}$$

The last step above is derived using a change of variables from ϕ_f to ϕ_n with J being the Jacobian of the map. The contraction algorithm samples the integral using the integrand on the RHS of the expression above. The integrand is not real, so the sampling is done based on the Boltzmann factor $\exp[-S_{\text{eff}}(\phi_n)]$ with

$$\begin{aligned} S_{\text{eff}}(\phi_n) &\equiv \text{Re}[S(\phi_f(\phi_n)) - \log\det J] \\ &= S_R(\phi_f(\phi_n)) - \log|\det J| \,. \end{aligned} \tag{2.11}$$

The phase $\varphi(\phi_n) \equiv S_I(\phi_f(\phi_n)) - \text{Im}\log\det J$ is reweighted as in Eq. 2.3. When $T_{\text{flow}} = 0$ the integration manifold is unchanged and the phase of the integrand fluctuates rapidly since the original formulation has a sign problem. As T_{flow} increases, S_R increases and the sampled points concentrate on ever smaller regions of the flowed manifold where S_R is small. As these regions are small and S_I is preserved by the flow, the phase fluctuations on these small sampled regions are also small, alleviating the sign problem. In the $T_{\text{flow}} \to \infty$ limit, these sampled regions reduce to isolated points, one for each contributing thimble. On the flowed manifold, for large T_{flow} , the regions with an important statistical weight form isolated pockets with particularly small S_R, each one corresponding to a particular contributing thimble. In this formulation, the full value of the integral is recovered only when all the pockets are sampled, corresponding to the inclusion of all thimbles appearing in the decomposition. Algorithms involving incremental changes in the field configurations will only sample the pocket closest to the starting configuration. This is actually how we employ our algorithm when we are interested in sampling only the contribution of one thimble. If we want to include the contribution of other thimbles we have to also make proposals that can take us from one pocket to another. We used this type of large updates previously in a fermionic model [5], and in Section IV we will present a similar procedure for the model we study in this paper.

The contraction algorithm is simply a Metropolis algorithm using the variables ϕ_n based on the effective action $S_{\text{eff}}[\phi_f(\phi_n))]$. The proposals have to be chosen carefully to get a reasonable acceptance rate. A number of optimizations are possible when the starting manifold $\mathcal{M}_n$ is not the original integration domain but the tangent manifold to a thimble of interest. This manifold is a legitimate choice in two cases: either we are interested in sampling only one thimble in the limit $T_{\text{flow}} \to \infty$ [2], or the tangent space to the thimble is equivalent to the original integration domain, which is the case for a class of systems. It was conjectured that this is also true for the model studied in this paper [12]. We will show evidence supporting this conjecture.

There are two advantages to using the tangent space of a critical point as the starting manifold instead of $\mathbb{R}^n$: we can make efficient Metropolis proposals [2] and we can use an estimator to take into account the contribution of the Jacobian to the effective action [14]. The Jacobian can be computed exactly by integrating the following differential equation along the upward flow path,

$$\frac{dJ}{dt} = \overline{HJ} \,, \tag{2.12}$$

where J is the Jacobian matrix and H is the Hessian of the action S. The initial condition for J is a matrix that has as columns a set of vectors that span the tangent space at the critical point. We use $J(0) = (\hat\rho_1, \ldots, \hat\rho_n)$, where $\hat\rho_i$ are the positive "eigenvectors" of the Hessian at the critical point, that is $\overline{H_0 \hat\rho_i} = \lambda_i \hat\rho_i$ with $\lambda_i > 0$. It can be shown that these vectors span the tangent space to the thimble $\mathcal{T}$ and that $i\hat\rho_i$ are negative "eigenvectors" that span the tangent space to the unstable thimble $\mathcal{K}$. Integrating the equation above is numerically expensive, since every step of the integrator involves multiplication of H and J matrices. Fortunately, there is a very good estimator for $\log|\det J|$ built out of the "eigenvectors"

$\hat{\rho}_i$ [14]:

$$W = \int_0^{T_{\rm flow}} dt \sum_{i=1}^{n} \hat{\rho}_i^\dagger \overline{H(t)\hat{\rho}_i}\,. \tag{2.13}$$

Since H is sparse, the cost of computing W is $\mathcal{O}(n)$, which is much cheaper than the $\mathcal{O}(n^2)$ cost of computing J; the savings are substantial even for small lattices. The algorithm samples configurations with an effective action $S'_{\rm eff}(\phi_n) = S_R(\phi_f(\phi_n)) - \mathrm{Re}\, W$ and the difference $\Delta S = S_{\rm eff}(\phi_n) - S'_{\rm eff}(\phi_n)$ is included as a reweighting factor. To compute the reweighting factor exactly we need to integrate the equations for J, but this needs to be done only for the small subset of configurations used for measuring observables, which are separated by a large number of Metropolis steps.

III. RELATIVISTIC BOSE GAS AT FINITE DENSITY

The Euclidean action of a gas of relativistic spinless bosons in three (spatial) dimensions at finite density is given by

$$\begin{aligned} S = \int d^4x \,\big[&\partial_0\phi^*\partial_0\phi + \nabla\phi^*\cdot\nabla\phi + (m^2-\mu^2)|\phi|^2 \\ &+ \mu \underbrace{(\phi^*\partial_0\phi - \phi\partial_0\phi^*)}_{j_0(x)} + \lambda|\phi|^4\big] \end{aligned} \tag{3.1}$$

where $\phi \equiv (\phi_1 + i\phi_2)/\sqrt{2}$ is a complex scalar field. The term involving the boson density $j_0(x)$ is imaginary and is the source of the sign problem in this model. This action is symmetric under global $U(1)$ transformations $\phi \to e^{i\alpha}\phi$. For values of μ below a critical value of order m the equilibrium state is expected to be $U(1)$ symmetric and $\langle\phi\rangle = 0$. For values of μ larger than the critical value and for low enough temperatures the $U(1)$ symmetry is expected to be spontaneously broken and $\langle\phi\rangle \neq 0$.

In order to study spontaneous symmetry breaking it is necessary to introduce an *explicit* symmetry breaking term $S \to S - h\int d^4x\,(\phi_1+\phi_2)$. This choice breaks the original $U(1)$ symmetry down to the $\mathbb{Z}_2$ sub-group given by swapping $\phi_{x,1} \leftrightarrow \phi_{x,2}$.

We use the following discretization of the action:

$$\begin{aligned} S = a^4 \sum_x \Bigg[&\frac{e^{\mu a}\phi^*_{x+\hat{0}} - \phi^*_x}{a}\frac{e^{-\mu a}\phi_{x+\hat{0}} - \phi_x}{a} \\ &+ \sum_{\nu=1}^{3}\left|\frac{\phi_{x+\hat{\nu}} - \phi_x}{a}\right|^2 + m^2|\phi_x|^2 \\ &+ \lambda|\phi_x|^4 \;- h(\phi_{x,1}+\phi_{x,2})\Bigg]\,. \end{aligned} \tag{3.2}$$

Setting the lattice spacing to $a = 1$ and writing the field in terms of real components, ϕ_1 and ϕ_2, we obtain

$$\begin{aligned} S = \sum_x \Bigg[&\Big(4 + \frac{m^2}{2}\Big)\phi_{x,a}\phi_{x,a} - \sum_{\nu=1}^{3}\phi_{x,a}\phi_{x+\hat{\nu},a} \\ &- \cosh\mu\;\phi_{x,a}\phi_{x+\hat{0},a} + i\sinh\mu\;\epsilon_{ab}\phi_{x,a}\phi_{x+\hat{0},b} \\ &+ \frac{\lambda}{4}(\phi_{x,a}\phi_{x,a})^2 - h(\phi_{x,1}+\phi_{x,2})\Bigg] \end{aligned} \tag{3.3}$$

with ϵ_{ab} the antisymmetric tensor with $\epsilon_{12} = 1$. The derivatives of the action are

$$\begin{aligned} \frac{\partial S}{\partial\phi_{x,a}} =&(8+m^2)\phi_{x,a} - \sum_{\nu=1}^{3}(\phi_{x+\hat{\nu},a} + \phi_{x-\hat{\nu},a}) \\ &- \cosh\mu\left(\phi_{x+\hat{0},a} + \phi_{x-\hat{0},a}\right) \\ &+ i\sinh\mu\epsilon_{ac}\left(\phi_{x+\hat{0},c} - \phi_{x-\hat{0},c}\right) \\ &+ \lambda(\phi_{x,c}\phi_{x,c})\phi_{x,a} - h\,, \\ \frac{\partial^2 S}{\partial\phi_{x,a}\partial\phi_{y,b}} =&(8+m^2)\delta_{xy}\delta_{ab} - \sum_{\nu=1}^{3}(\delta_{x+\hat{\nu},y} + \delta_{x-\hat{\nu},y})\,\delta_{ab} \\ &- \cosh\mu\left(\delta_{x+\hat{0},y} + \delta_{x-\hat{0},y}\right)\delta_{ab} \\ &+ i\sinh\mu\left(\delta_{x+\hat{0},y} - \delta_{x-\hat{0},y}\right)\epsilon_{ab} \\ &+ \lambda\delta_{xy}\left[(\phi_{x,c}\phi_{x,c})\delta_{ab} + 2\phi_{x,a}\phi_{x,b}\right]\,. \end{aligned} \tag{3.4}$$

It is very difficult to find all critical points of the (latticized) action. However, critical points with small S_R play a special role as their thimbles are more likely to dominate the path integral. Critical points with constant fields $\phi_{xa} = \phi$ are among the ones with smaller values of the action and, at the same time, are easy to find. In fact, the global minimum of the real part of the action restricted to real values of $\phi_{x,1}$ and $\phi_{x,2}$ is a constant field (assuming h real). This can be seen by looking at Eq. 3.1 or its discretized version Eq. 3.2 and noticing that i) the kinetic and gradient term are positive definite and favor constant fields and ii) the term linear in μ is purely imaginary and does not contribute to the real part of the action. This motivates us to find the constant field critical points. They are given by $\phi_{x,1} = \phi_{x,2} = \phi$ where ϕ is one of the roots of the cubic equation:

$$(2+m^2)\phi - 2\cosh\mu\phi + \lambda|\phi|^2\phi = h, \tag{3.5}$$

whose three solutions are given, for small h, by:

$$\begin{aligned} \phi_0 &= -\frac{h}{\hat{\mu}^2 - m^2} + \mathcal{O}(h^2)\,, \\ \phi_\pm &= \pm\sqrt{\frac{\hat{\mu}^2 - m^2}{2\lambda}} + \frac{h}{2}\frac{1}{\hat{\mu}^2 - m^2} + \mathcal{O}(h^2), \end{aligned} \tag{3.6}$$

with $\hat{\mu}^2 = 2\cosh\mu - 2$. The corresponding values of the

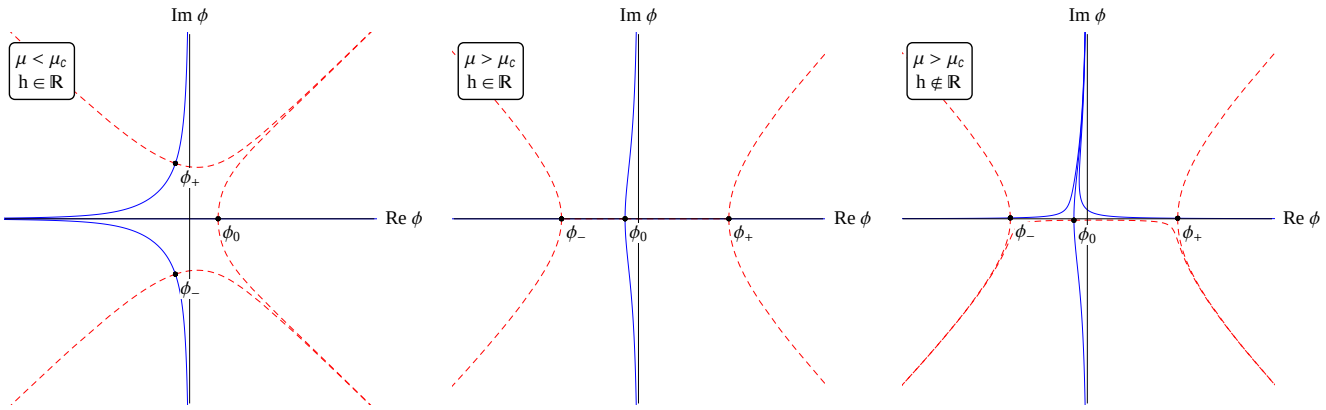

FIG. 1. Projections in the constant $\phi_1 = \phi_2$ subspace for $\mathcal{T}_0$, $\mathcal{T}_+$ and $\mathcal{T}_-$, the thimbles attached to ϕ_0, ϕ_+ and ϕ_-. The left and middle graph correspond to h real and the one on the right to a value of h that has a small imaginary component. Thimbles $\mathcal{T}_i$ are plotted in blue, unstable thimbles $\mathcal{K}_i$ are plotted with dashed, red lines, and critical points are indicated by black dots.

action at these points are:

$$\begin{aligned}\frac{S(\phi_0)}{V_4} &= 0 + \mathcal{O}(h^2)\,,\\ \frac{S(\phi_\pm)}{V_4} &= -\frac{1}{\lambda}\left(\frac{\hat{\mu}^2 - m^2}{2}\right)^2 \mp 2h\sqrt{\frac{\hat{\mu}^2 - m^2}{2\lambda}} + \mathcal{O}(h^2)\,,\end{aligned} \tag{3.7}$$

where $V_4 = (V/a^3)/(aT)$ is the number of lattice sites.

We now turn to discuss what we know about the thimble decomposition of the original integral over real fields. For μ below $\mu_c = \cosh^{-1}(1 + m^2/2)$ the critical points $\phi_\pm$ are imaginary. In this case the thimbles $\mathcal{T}_\pm$ associated with $\phi_\pm$ do not contribute to the thimble decomposition. This is because the real part of the action in $\mathbb{R}^n$ is bounded from below by $\mathrm{Re}\, S(\phi_0)$ which is larger than $\mathrm{Re}\, S(\phi_\pm)$. Thus no point in the original integration domain can flow into $\phi_\pm$ under steepest-ascent/upward-flow defined in Eq. 2.9. This is illustrated in the the left panel of Fig. 1 which shows a projection of the thimbles $\mathcal{T}_{0,\pm}$ in the $\phi_1 = \phi_2$ plane. We can see that, in the $\mu < \mu_c$ case, the unstable thimbles $\mathcal{K}_\pm$ do not intersect the original integration domain, which is the real axis in this figure.

For values of μ greater than μ_c the situation changes. In the case where $\mu > \mu_c$ and h is real, there is a trajectory of the flow connecting ϕ_0 and ϕ_+ (ϕ_-). Indeed, in the constant field subspace (that is, in the subspace where $\phi_{x,1} = \phi_{x,2} = \phi$) the gradient

$$\left.\frac{\partial S}{\partial \phi_{x,a}}\right|_{\phi_{x,1}=\phi_{x,2}=\phi} = (m^2 - \hat{\mu}^2)\phi + 2\lambda\phi^3 - h \tag{3.8}$$

points along the constant field subspace (all components are equal). Moreover, the gradient is real if ϕ is real. This implies in the existence of flow trajectories lying entirely on the real constant field subspace. Since the downward flow decreases the value of the real part of the action, we conclude that there is a trajectory connecting the real constant fields ϕ_0 and ϕ_+ (and another connecting ϕ_0 to ϕ_-). Thus, the unstable thimble of ϕ_0 ($\mathcal{K}_0$) overlaps the thimble of ϕ_+ ($\mathcal{T}_+$). The existence of these lines is known as a Stokes phenomenon and invalidates the decomposition of the integral into integer linear combinations of thimbles. We bypass this problem by making h slightly complex. As can be seen from Eq. 3.7 a complex value of h implies different values for the imaginary parts of $S(\phi_+), S(\phi_-)$ and $S(\phi_0)$. As the flows preserves the imaginary part of the action, a complex value of h guarantees that there is no Stokes lines connecting these critical points. The way a complex value of h makes the thimble decomposition well defined is shown visually in the center and right panels of Fig. 1. The figure suggests that the integral over the real line is equivalent to the integral over $\mathcal{T}_+$ and $\mathcal{T}_-$ (with the proper orientations), which would imply that $n_+ = n_- = 1, n_0 = 0$. The Fig. 1 only shows a projection of the whole space but some definite conclusions can be drawn. For instance, the fact that there is a flow line connecting the real plane to ϕ_- shows that $\mathcal{K}_-$ does intersect $\mathbb{R}^n$, although the possibility remains that there are other (non-constant field) points where $\mathcal{K}_-$ intersects $\mathbb{R}^n$. This is a strong but not definitive case that $n_- = 1$. The fact that $n_+ = 1$ can be argued even more rigorously. The difference in the real part of the action between ϕ_+ and the global minimum on the real plane is proportional to $\mathrm{Im}(h)$. In the $\mathrm{Im}(h) \to 0$ limit this region shrinks to a point [18] showing that, at least in this limit, $n_+ = 1$. To the extent that the constant field projection can be trusted we also have $n_0 = 0$. Unfortunately, the picture away from the constant field subspace is much harder to analyze and there is the possibility that $\mathcal{T}_0$, or even that thimbles corresponding to other, non-constant field critical points, may also contribute. Even if the unstable thimble $\mathcal{K}_0$ were to intersect the real integration domain at a point not included in the projection in Fig. 1, and therefore contribute to the thimble decomposition of the

original integral, its contribution is expected to be much smaller than the one from $\mathcal{T}_-$. In fact, the leading order estimate (in the semiclassical expansion) for the relative contribution of two thimbles, say $\mathcal{T}_0$ and $\mathcal{T}_+$, is given by the ratio of Boltzmann factors $\exp(-[S(\phi_0) - S(\phi_+)])$. Since the difference in the action at ϕ_0 and ϕ_+ is approximately $(\hat{\mu}^2 - m^2)^2/4\lambda$, the contribution of $\mathcal{T}_0$, if not identically zero, is exponentially small as $V_4 \gg 1$ (or $\hat{\mu} \gg m$ or $\lambda \ll 1$).

The last topic to discuss in this section is the evaluation of the estimator in Eq. 2.13. This is done by integrating the differential equation

$$\frac{dW}{dt} = \mathrm{Tr}\,' H \quad \text{with} \quad \mathrm{Tr}\,' H \equiv \sum_i \hat{\rho}_i^\dagger \overline{H(\phi(t))\hat{\rho}_i} \tag{3.9}$$

together with the upward flow in Eq. 2.9. These differential equations are integrated using a Cash-Karp integrator, an adaptive step-size integrator of order $\mathcal{O}(\Delta t^5)$ [19]. For every integrator step we need to evaluate $\mathrm{Tr}\,' H(\phi(t))$, which requires the positive "eigenvectors" $\hat{\rho}_i$ for the Hessian at the critical point $\phi_{\rm cr}$

$$\overline{H(\phi_{\rm cr})\hat{\rho}_i} = \lambda_i \hat{\rho}_i\,, \quad \text{with} \quad \lambda_i > 0\,, \tag{3.10}$$

where

$$H(\phi)_{x,a;y,b} = \frac{\partial^2 S}{\phi_{x,a}\phi_{y,b}}\,, \quad \text{and} \quad \hat{\rho}_i^\dagger \hat{\rho}_j = \delta_{ij}\,. \tag{3.11}$$

We stress that the estimator involves only the "eigenvectors" of the Hessian at the critical point and not the ones of $H(\phi)$. This estimator is exact when the action is quadratic and it tracks well the true value of the Jacobian even when the thimble is curved [14]. We compute the "eigenvectors" before starting the Monte-Carlo simulation. This step is computationally costly but needs to be performed only once. To evaluate the estimator, we separate the ϕ-dependent part from the Hessian as:

$$\begin{aligned} H(\phi)_{x,a;y,b} =& H(\phi_{\rm cr})_{x,a;y,b} + \lambda\delta_{xy}\big[(\phi_{x,c}\phi_{x,c})\delta_{ab} \\ &+ 2\phi_{x,a}\phi_{x,b} - (\phi \to \phi_{\rm cr})\big]\,. \end{aligned} \tag{3.12}$$

We have then

$$\begin{aligned} \mathrm{Tr}\,' H(\phi) &= \mathrm{Tr}\,' H(\phi_{\rm cr}) + \overline{\Delta(\phi)} - \overline{\Delta(\phi_{\rm cr})} \\ &= \left(\sum_i \lambda_i - \overline{\Delta(\phi_{\rm cr})}\right) + \overline{\Delta(\phi)}\,, \end{aligned} \tag{3.13}$$

where we used the fact that $\mathrm{Tr}\,' H(\phi_{\rm cr}) = \sum_i \lambda_i$ and the definitions

$$\begin{aligned} \Delta(\phi) &\equiv \sum_x \sum_{abc} \mathcal{R}_{x,ab}\left[\phi_{x,c}\phi_{x,c}\delta_{ab} + 2\phi_{x,a}\phi_{x,b}\right]\,, \\ \mathcal{R}_{x,ab} &\equiv \sum_i (\hat{\rho}_i)_{x,a}(\hat{\rho}_i)_{x,b}\,. \end{aligned} \tag{3.14}$$

Note that $\mathrm{Tr}\,' H(\phi_{\rm cr})$, $\Delta(\phi_{\rm cr})$, and $\mathcal{R}$ are computed once at the beginning of the simulation and we only need to evaluate $\Delta(\phi)$ along the integration path. This step has computational cost of order $\mathcal{O}(n)$.

IV. RESULTS

In this section we present the results of our simulations. We discuss first the exact results, based on simulations on the thimble tangent plane at the ϕ_+ critical point, both in the symmetric and the broken phase. We then focus on the broken phase and analyze the dependence of the order parameter as a function of the breaking parameter h to determine the regime where finite volume effects are not dominant. After that we report the results of single thimble simulations on the dominant thimble, $\mathcal{T}_+$, and compare them with exact results. Finally, we present a method to carry out simulations on two thimbles and study the relative weight of $\mathcal{T}_-$ to $\mathcal{T}_+$ as a function of h.

As we discussed in Section II, we can use the contraction algorithm to get exact results by flowing the original domain of integration $\mathbb{R}^n$. However, if the starting manifold is the tangent space at the critical point on a thimble then shorter flow times are required to reduce the phase fluctuations and we can use better proposals for the Metropolis algorithm and fast Jacobian estimators. This choice is justified if we can show that this manifold is equivalent with the original integration domain. Cristoforetti *et al* [12] conjectured this to be the case for the relativistic Bose gas: they argue that the original integration domain is equivalent to the tangent space for the thimble corresponding to the global minimum of S_R over $\mathbb{R}^n$. They use real values of h and the global minimum corresponding to the constant field critical point ϕ_0 for $\mu < \mu_c$ and ϕ_+ for $\mu \geq \mu_c$. Note that the transition from ϕ_0 to ϕ_+ is smooth since they are equal for $\mu = \mu_c$. The manifolds T_0 and T_+ are the tangent manifolds to the thimbles $\mathcal{T}_0$ and $\mathcal{T}_+$ at the critical points ϕ_0 and ϕ_+ respectively. Note that when using a slightly complex h, as we use, the points ϕ_0 and ϕ_+ have small complex components, proportional to $\mathrm{Im}\, h$. The tangent spaces T_0 and T_+ are not parallel to $\mathbb{R}^n$, even in the limit $h \to 0$, so an analytical proof of the conjectured equivalence cannot be easily established.

We carried out simulations using $T_{\rm flow} = 0$ using as the starting manifold T_0 for $\mu < \mu_c$ and T_+ for $\mu \geq \mu_c$. To make sure that we stay on the manifold we determine the "eigenvectors" $\hat{\rho}_i$ and parametrize each point on the manifold as $\phi = \phi_{\rm cr} + \sum_i c_i \hat{\rho}_i$, where c_i are real coefficients. We use c_i to represent the points in the tangent space, and the updates are done one coefficient at a time with a step drawn from an uniform probability distribution in the interval $[-\theta, \theta]$ where $\theta = \Delta/\sqrt{\lambda_i}$. This type of proposal scales the step size in each direction so that the increase in the action due to displacements in each direction are comparable, at least in the region where the action is well approximated by its quadratic approximation around $\phi_{\rm cr}$. We tune Δ to get a good acceptance rate. In Fig. 2 we

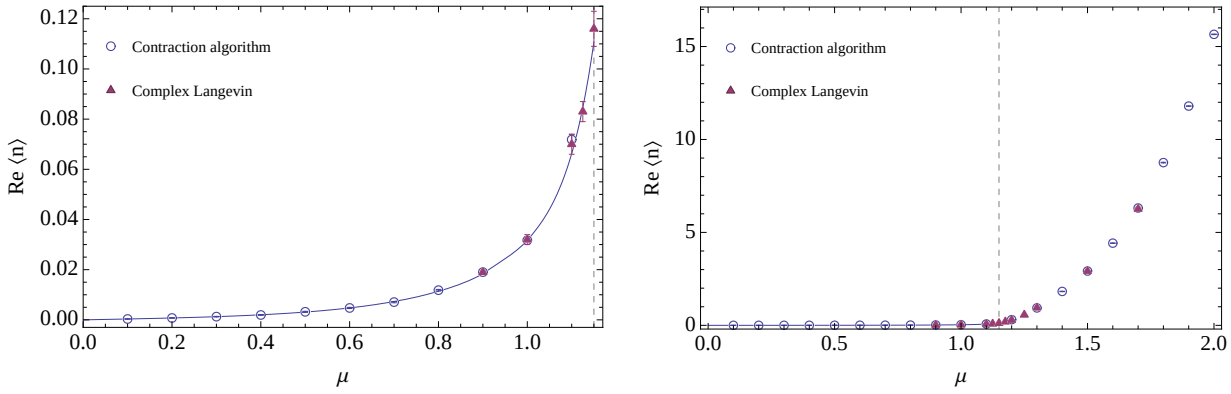

FIG. 2. Dependence of the charge $\mathrm{Re}\,\langle n\rangle$ on the chemical potential on a 4^4 lattice with parameters $m = \lambda = 1.0$ and $h = 10^{-3} + i10^{-4}$. In the left panel we plot only the data below $\mu_c^{\mathrm{mean}} \approx 1.15$, the mean field estimate for the transition to the symmetry broken phase [9]. Complex Langevin data is taken from [6] and the curve in the left panel from a mean field calculation that is known to agree very well with exact results results [9].

show the results for the charge

$$\begin{aligned}\langle n\rangle &= \frac{1}{V_4}\frac{\partial \log Z}{\partial \mu} \\ &= \frac{1}{V_4}\sum_x (\delta_{ab}\sinh\mu - i\epsilon_{ab}\cosh\mu)\phi_{x,a}\phi_{x+\hat{0},b}\,.\end{aligned} \tag{4.1}$$

In these simulations we set $h = 10^{-3} + i10^{-4}$ and $\Delta = 3.0$ so that the acceptance rate was close to 50%. For each value of μ we evaluated 5×10^6 updates and performed measurements on configurations separated by 1000 updates. We compare our results with the results from Complex Langevin simulations [6], which are known to agree with the results obtained from the dual variables approach [7]. Our results agree very well which strongly supports the conjecture that the tangent plane is equivalent with the original integration domain. We note that we observed neither instabilities nor runaways in our simulations, in contrast with the experiences reported by Cristoforetti *et al* [12], even when we set h to purely real values, as they did in their study.

The simulations above are feasible even at $T_{\mathrm{flow}} = 0$ because the sign fluctuations are significantly smaller when integrating over the tangent space rather than the original integration domain. In Fig. 3 we show the average phase, $\mathrm{Re}\left\langle \mathrm{e}^{-iS_I}\right\rangle$, and its standard deviation as a function of the chemical potential in the symmetric phase, both for simulations using $\mathbb{R}^n$ as a starting manifold and T_0. We show in the graph both the standard deviation and the standard deviation of the mean of $\mathrm{Re}\left\langle \mathrm{e}^{-iS_I}\right\rangle$ so that the number of sampled points in the simulations do not play a role in the comparison. We see that as we approach the transition point, the phase fluctuates rapidly when we sample points on $\mathbb{R}^n$ and the number of sampled configurations required to measure the observables with a given precision grows very quickly. In contrast, the phase fluctuations on T_0 are very mild, at least for the lattice volume used in these simulations, and the phase can be easily accounted for by reweighting.

As discussed earlier, when the symmetry breaking parameter h goes to zero, the order parameter

$$\langle\phi\rangle = \frac{1}{V_4}\frac{\partial \log Z}{\partial h}\,, \tag{4.2}$$

vanishes if the limit $h \to 0$ is taken while the volume is kept fixed. In the symmetry broken phase, this is a finite volume effect. This happens because when h is small the fluctuations in ϕ are large enough to overcome the potential barrier between ϕ_+ and ϕ_-, $\Delta S = V_4 4h\sqrt{(\hat{\mu}^2 - m^2)/(2\lambda)} + \mathcal{O}(h^2)$. Since we discuss here simulations at fixed volume, it is important to determine the range of h where these finite volume effects

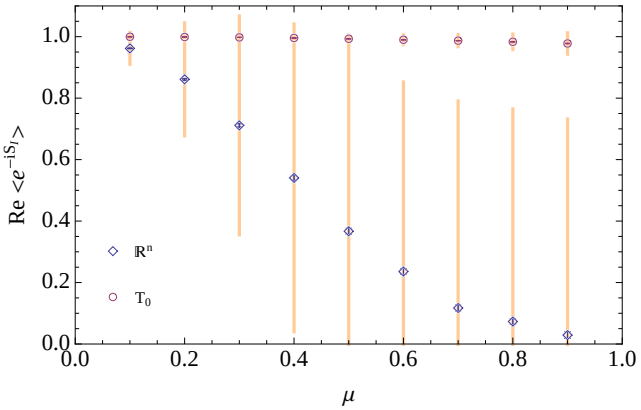

FIG. 3. Dependence of the average phase on the chemical potential μ below the critical transition on the real plane and the tangent plane T_0 for a 4^4 lattice with the parameters $m = \lambda = 1.0$. The orange bars indicate the standard deviation of $\mathrm{Re}\, e^{-iS_I}$. The phase hardly varies for these parameters, so in this case it is sufficient to shift the integration domain to T_0 to tame the sign problem.

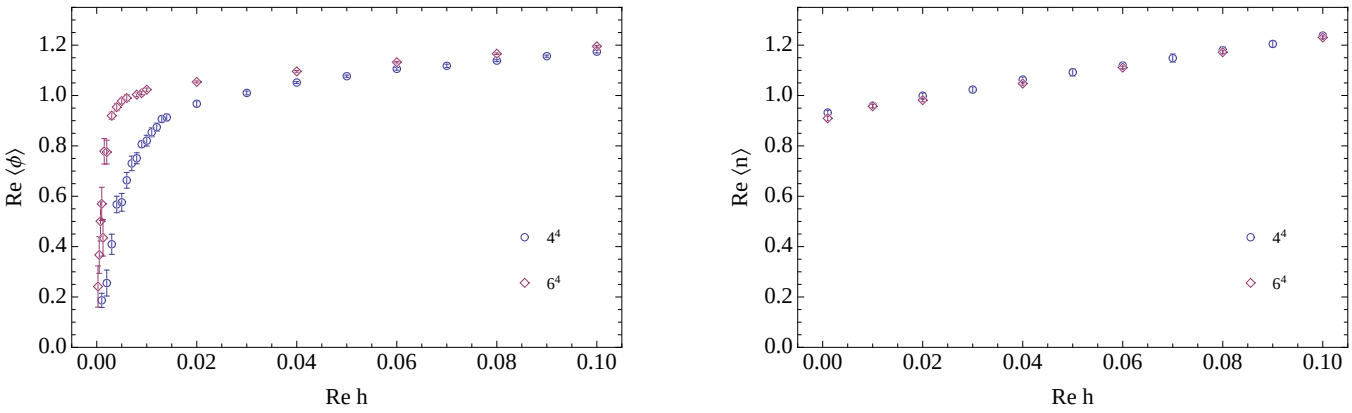

FIG. 4. Observables as a function of the symmetry breaking parameter h on a 4^4 lattice (blue) and 6^4 lattice (red) with $m = \lambda = 1.0$, $\mu = 1.3$. Note that the charge varies slowly as we decrease h, whereas for $\mathrm{Re}\, h \lesssim 0.02$ the order parameter $\langle\phi\rangle$ becomes dominated by finite volume effects and, as expected, approaches zero as $h \to 0$. As expected, the values of h for which there is a significant finite volume effect decreases as the volume is increased.

are important. In Fig. 4 we plot the charge and the order parameter $\langle\phi\rangle$ as a function of h, as determined from simulations over T_+. We set the value of the chemical potential to $\mu = 1.3$, to make sure we are in the high-density, symmetry broken phase. In these simulations the ratio between the imaginary and real part of h is kept fixed: $\mathrm{Re}\, h/\,\mathrm{Im}\, h = 10$. We see that for values smaller than $\mathrm{Re}\, h \lesssim 0.02$ (for the 4^4 lattice) and $\mathrm{Re}\, h \lesssim 0.01$ (for the 6^4 lattice) the finite volume effects become important and restore the (near) symmetry. For the following calculation we use a value of $h = 0.1 \times (1 + i/10)$ to make sure we are away from the region where finite volume effects dominate.

Note that for these simulations, at small values of h, there is a nearly flat direction in field space that is sampled inefficiently using the proposals discussed earlier. This can be easily fixed. The flat direction corresponds roughly to a circle in the two-dimensional space spanned by $\hat{\rho}_0$, the "eigenvector" nearly parallel with the constant field with $\phi_1 = -\phi_2$ (the "Goldstone" direction) and "eigenvector" $\hat{\rho}_1$ nearly parallel with the constant field direction with $\phi_1 = \phi_2$ (the "Higgs" direction). The updates along the other directions are treated as discussed above, but in the $\hat{\rho}_{0,1}$ plane we use a polar representation and update the angular part with steps of size $\Delta/\sqrt{\lambda_0}$ and the radial part with steps of size $\Delta/\sqrt{\lambda_1}$. The polar coordinates are defined in relation to the center $c_0 = 0$ and $c_1 = (\phi_- - \phi_+) \cdot \hat{\rho}_1/2$, with $c_{0,1}$ the coordinates in the $\hat{\rho}_{0,1}$ basis. To preserve detailed balance we have to modify the accept/reject step to take into account the asymmetry in this polar proposal, that is we accept the update with probability $\exp[-S_R(\phi') + S_R(\phi)]r'/r$, where r and r' represent the radial coordinates for ϕ and ϕ' in the polar representation.

As we discussed in Section III, to obtain exact results for this model using thimble sampling we have to consider a set of thimbles, at the very least $\mathcal{T}_+$ and $\mathcal{T}_-$. One of the questions we want to address here is whether the single thimble calculation is sufficient to recover the exact result. Note that previous calculations for the relativistic boson gas that used Lefschetz thimbles were either carried out in the tangent plane [12], which as we argued provides the exact result, or without including the symmetry breaking term in which case the critical point is actually a circle and the integration was done over the entire set of thimbles attached to this circle [13]. As such, this question has not yet been directly addressed.

In Section II we showed that to perform a one thimble calculation with the contraction algorithm, say $\mathcal{T}_\sigma$, we need to sample the manifold produced by flowing the tangent space of the thimble at the critical point T_σ, in the limit $T_{\rm flow} \to \infty$. If we start at the critical point ϕ_σ and perform only small step updates, for large flow times the algorithm will only sample $\mathcal{T}_\sigma$. We focus here on the symmetry broken phase and we carry out a simulation for $\mu = 1.3$. The thimble we sample is $\mathcal{T}_+$. As the limit $T_{\rm flow} \to \infty$ cannot be taken in practice, it is necessary to devise an operational definition. We carry out simulations at increasing flow times and monitor the observables of interest and the imaginary part of the action on the sampled manifold. As the sampled manifold approaches the thimble the observables should converge to their average over the thimble and the fluctuations of the imaginary part of the action around $S_I(\phi_+)$ should be reduced drastically in amplitude (in the limit $T_{\rm flow} \to \infty$ all points in the sampled pocket around ϕ_+ should have the same S_I).

We carried out simulations for $\mu = 1.3$, $h = 0.1 \times (1 + i/10)$ and measured the order parameter and the charge as a function of $T_{\rm flow}$. For each simulation we carried out 5×10^6 updates and we adjusted the step size to get an acceptance rate close to 50%. Note that the step size needs to be decreased dramatically, since the updates are carried out in the parametrization manifold, where the distribution of configurations become tightly packed

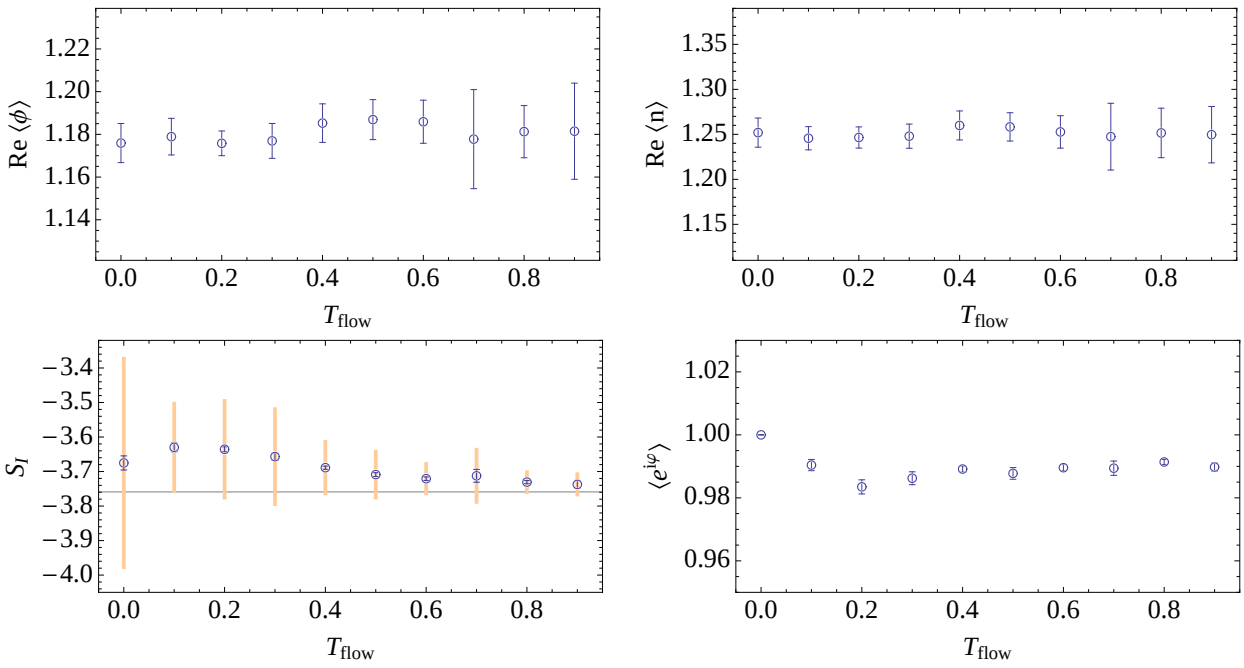

FIG. 5. T_{flow} extrapolations for the order parameter and the charge (top row) and the average imaginary part of the action $S_I(\phi_f)$ and the residual phase $\exp i\varphi = d\phi/|d\phi|$ which is computed as $\varphi = \operatorname{Im}\log\det J$ (bottom row) on a 4^4 lattice with $m = \lambda = 1.0$, $h = 0.1(1 + i/10)$, and $\mu = 1.3$. For S_I we also indicate the standard deviation to gauge its fluctuations.

around the critical point. We have to use anisotropic proposals along the "eigenvectors" in the tangent plane to take into account the fact that the flow compresses these directions differently, which is done by adjusting the step size in direction $\hat{\rho}_i$ to $\Delta \exp(-\lambda_i T_{\text{flow}})/\sqrt{\lambda_i}$ [2]. The measurements were carried out on configurations separated by 10,000 updates.

In Fig. 5 we show our results. We see that the values of $\langle\phi\rangle$ and $\langle n\rangle$ show very little dependence on the flow time, indicating that the single thimble result is equal to the exact result, at least at the level of the errobars. In the bottom row of the figure we also plot the value of the imaginary part of the action for the configurations sampled in our Monte Carlo simulations. It is clear that the fluctuations die out quite quickly, and as T_{flow} approaches 1.0 we have almost no fluctuations, indicating that we are sampling $\mathcal{T}_+$ only. In the bottom left panel of Fig. 5 we plot the residual phase, that is the phase related to the curvature of the sampled manifold, as a function of flow time. In our formulation, this is the part of the reweighting phase that is due to the imaginary part of the Jacobian, that is $\operatorname{Im}\log\det J$. In the limit $T_{\text{flow}} \to \infty$ the fluctuations of S_I vanish, but the residual phase continues to fluctuate. These fluctuations are not expected to lead to a sign problem, since the thimbles are expected to be relatively smooth at least in the region where the bulk of the contribution to the integral comes from. This is indeed what we find: the phase fluctuations are very close to one for all intermediate manifolds and asymptote to $\langle\exp(i \operatorname{Im}\log\det J)\rangle = 0.989(1)$. The closeness of this average to 1 also indicates that the thimble is quite flat. Incidentally, our result for the average residual phase is in agreement with the one determined by Fujii *et al* [13] for $\mu = 1.3$ using the HMC algorithm: $\langle\exp(i \operatorname{Im}\log\det J)\rangle = 0.99(3)$. Note that they sample a different manifold than $\mathcal{T}_+$ ($h = 0$ in that calculation), so it is not clear that a geometric measure like the average residual phase should be identical.

We conclude that in the regime where the finite volume effects are small, the partition function is dominated by the contribution of one thimble $\mathcal{T}_+$. However, it is still worthwhile investigating the contribution due to other thimbles for two reasons. First, if we are interested in studying the system when the symmetry breaking term is small and the finite volume effects are important, it is likely that we need to include the contribution from other thimbles. Secondly, while we showed that the two observables we measured seem to be saturated by the contribution of $\mathcal{T}_+$, it is possible that these observables are special in the sense of being insensitive to removing the samples due to other thimbles.

Semiclassical arguments suggest the contribution of subdominant thimbles vanishes. If we consider the ratio of the two contributions to the partition function

$$\frac{Z_+}{Z_-} \equiv \frac{\int_{\mathcal{T}_+} |d\phi|\, e^{-S_R(\phi)}}{\int_{\mathcal{T}_-} |d\phi|\, e^{-S_R(\phi)}} \tag{4.3}$$

we expect that it goes to infinity very quickly as $\mathrm{Re}\, h$ increases. At leading order in the semiclassical expansion this ratio is

$$\frac{Z_+}{Z_-} \approx e^{-[S_R(\phi_+)-S_R(\phi_-)]} \approx e^{4\mathrm{Re}\, h V_4 \sqrt{(\hat{\mu}^2-m^2)/(2\lambda)}}, \tag{4.4}$$

which justifies our expectation. The next-to-leading order estimate includes the gaussian fluctuations

$$\frac{Z_+}{Z_-} \approx e^{-[S_R(\phi_+)-S_R(\phi_-)]} \sqrt{\frac{\widetilde{\det} H(\phi_-)}{\widetilde{\det} H(\phi_+)}}, \tag{4.5}$$

with $H(\phi)$ the hessian at ϕ and $\widetilde{\det} H(\phi)$ being the product of positive "eigenvalues" λ_i as defined in Eq. 3.10. The next to leading order ratio increases more slowly than the leading order estimate and it is possible that the semiclassical arguments could break down. In the remainder of this section we will study numerically the relative contribution due to $\mathcal{T}_-$ and compare it with the semiclassical approximation.

We present here a method to sample two thimbles in the context of the contraction algorithm. Assuming that the original integration domain decomposes into a sum over $\mathcal{T}_+$ and $\mathcal{T}_-$, the average observable is given by

$$\langle \mathcal{O} \rangle = \frac{n_+ \int_{\mathcal{T}_+} d\phi\, e^{-S(\phi)} \mathcal{O}(\phi) + n_- \int_{\mathcal{T}_-} d\phi\, e^{-S(\phi)} \mathcal{O}(\phi)}{n_+ \int_{\mathcal{T}_+} d\phi\, e^{-S(\phi)} + n_- \int_{\mathcal{T}_-} d\phi\, e^{-S(\phi)}}. \tag{4.6}$$

Notice that both thimbles appear in both the numerator and the denominator, which makes a decomposition of $\langle \mathcal{O} \rangle$ into a straightforward sum of integrals over thimbles not possible. The integers n_+ and n_- count the number of intersection points between the parametrization manifold and the unstable thimbles $\mathcal{K}_+$ and $\mathcal{K}_-$. Each of them lies within a different pocket in the parametrization manifold. In our simulations on the tangent plane T_+ we have only seen evidence for one intersection point with $\mathcal{K}_+$ at ϕ_+ and one intersection point close to ϕ_- (ϕ_- is not included in T_+ but it is nearby), which we assume is associated with $\mathcal{K}_-$. Here we will discuss a method to sample only these two pockets, implicitly assuming that $|n_\pm| = 1$; the sign of $n_\pm$ is automatically taken into account correctly by the flow.

To sample $\mathcal{T}_+$ and $\mathcal{T}_-$ simultaneously, we use the contraction algorithm with large T_{flow} and set T_+ as the parametrization manifold, which we assume to be equivalent with $\mathbb{R}^n$. The only difference is that instead of starting close to ϕ_+ and making only small proposals, we interweave these updates with large proposals that move us from the vicinity of ϕ_+ to the neighborhood of ϕ_-. Since we parametrize the configurations in T_+ using coefficients in the $\hat{\rho}_i$-basis, we implement this proposal by flipping the sign of the coefficient corresponding to the eigenvector $\hat{\rho}_1$, that is nearly parallel with the constant field $\phi_1 = \phi_2$ configuration. In the limit that $T_{\mathrm{flow}} \to \infty$ this process will sample the two thimbles according to the probability density

$$\frac{d\mathrm{Pr}_\pm(\phi)}{|d\phi|} = e^{-S_R(\phi)} \Big/ \int_{\mathcal{T}_+ \cup \mathcal{T}_-} |d\phi|\, e^{-S_R(\phi)}. \tag{4.7}$$

As before, the residual phase needs to be folded in the observable in the reweighting step. Additionally, there is another fluctuating phase, even in the $T_{\mathrm{flow}} \to \infty$ limit, since the imaginary part of the action is different on the two thimbles ($S_I(\phi_+) \neq S_I(\phi_-)$). In the regime we study here, both these phases lead to mild fluctuation and there is no problem reweighting them.

Note that for computing the reweighting factor we do not need to identify the thimble associated with any of the sampled points. The flow automatically produces the right result. In fact, the identification might not even be possible for small T_{flow} since the separation into $\mathcal{T}_\pm$ contributions is not sharply defined. However, as we increase T_{flow} it is easy to identify the associated thimble

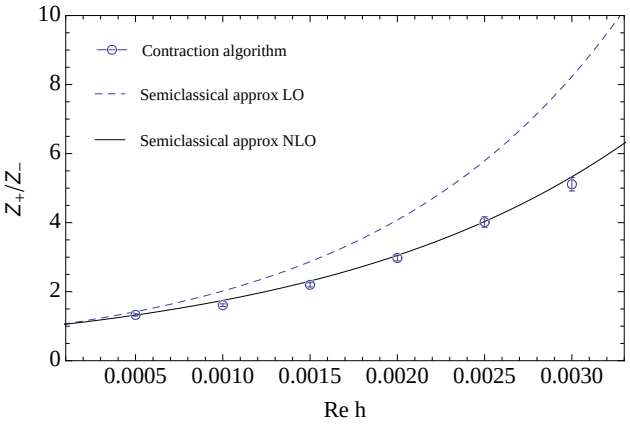

FIG. 6. The relative weights of thimble contribution as determined from sampling with the contraction algorithm, compared to the predictions from semiclassical approximation.

h_R	Z_1/Z_2	LO	NLO
5×10^{-4}	1.33(3)	1.42	1.32
10×10^{-4}	1.61(4)	2.02	1.75
15×10^{-4}	2.20(6)	2.87	2.31
20×10^{-4}	2.98(8)	4.08	3.05
25×10^{-4}	4.02(15)	5.79	4.03
30×10^{-4}	5.11(20)	8.23	5.33
0.02	$10^7/0$	1.27×10^6	6.96×10^5
0.1	$10^7/0$	2.67×10^{30}	1.01×10^{24}

TABLE I. Distribution of points among the two lowest action thimbles $\mathcal{T}_+$ and $\mathcal{T}_-$ over the course of a 10×10^6 step Monte Carlo on a 4^4 lattice with parameters $m = \lambda = 1.0$, $\mu = 1.3$, $T_{\mathrm{flow}} = 1.0$. For large values of h not a single transition occurs between $\mathcal{T}_+$ and $\mathcal{T}_-$ over the entire course of a Monte Carlo simulation. The results are compared with the leading order (LO) and next to leading order (NLO) semiclassical predictions.

for each of the configuration sampled in T_+ since they concentrate very sharply around $\phi_\pm$. We run a set of 10×10^6 updates for $\mu = 1.3$, $m = 1$, $\lambda = 1$ and a series of values for h, while we keep as before $\mathrm{Re}\, h / \mathrm{Im}\, h = 10$. We set $T_{\rm flow} = 1$, so that the associated thimble can be identified easily and the ratio of sampled points in $\mathcal{T}_+$ and $\mathcal{T}_-$ can be computed. The results are plotted in Fig. 6. We see that for small values of h, where $\mathcal{T}_-$ has a non-negligible contribution, this ratio is actually very close to the predictions of the next-to-leading order semiclassical approximation. We conclude that the non-gaussian fluctuations do not affect the sampling ratio significantly and that the semiclassical arguments can be trusted. In Table I we record the measured values for this ratio. We also include the results for two simulations with large values of h, similar to the ones we discussed earlier in this section, and we see that the subdominant thimble $\mathcal{T}_-$ is never visited, in agreement with semiclassical prediction. We conclude that for values of h where the finite volume effects are small, the subdominant thimbles are indeed unlikely to contribute significantly.

V. CONCLUSIONS

We analyzed the relativistic Bose gas using contraction algorithm, presenting the first application of the contraction algorithm to a quantum field theory. In studying the high density broken phase of the theory, we noticed the existence of a Stokes line and fixed this problem by using a complex value of the symmetry breaking parameter h. We verified that the results obtained for the charge density agreed with previous calculations when available. We then focused on the order parameter $\langle\phi\rangle$, which is sensitive to spontaneous symmetry breaking. We first determined the values of h for which finite volume effects, which tend to restore the symmetry, are small. The results from complex Langevin calculations agree with our tangent plane calculations, lending support to the conjecture that the tangent plane is indeed equivalent to the real plane. In contrast to [12] we found no runaway trajectories, as expected if the tangent plane is in fact equivalent to the real plane.

We then showed how to use the contraction algorithm to isolate the contribution of a single thimble. The results obtained from the single thimble agree with the results obtained from the tangent plane within a few percent, indicating that the contributions from other thimbles are negligible for the parameters explored. We generalized the contraction algorithm to perform calculations over two thimbles. We found that the contribution from the sub-dominant thimble follows closely the semiclassical estimates (negligible at large h but comparable to the leading one at smaller h).

Our calculations point towards some obvious extensions and generalizations. The most pressing one is perhaps the extension to the thermodynamic limit, with the goal of determining whether the contribution of any other thimble survives this limit. Also, our group has recently developed similar technology to that described in this paper to study the real time dynamics of a simple quantum mechanical model [20]. We look forward to combining the experience acquired in the present paper to study the real time dynamics of the Bose gas with an eye towards the computation of transport coefficients.

ACKNOWLEDGMENTS

A.A. is supported in part by the National Science Foundation CAREER grant PHY-1151648. A.A. gratefully acknowledges the hospitality of the Physics Department at the University of Maryland where part of this work was carried out. G.B., P.B., G.R and N.C.W. are supported by U.S. Department of Energy under Contract No. DE-FG02-93ER-40762.

[1] M. Cristoforetti, F. Di Renzo, and L. Scorzato (Aurora-Science), Phys. Rev. **D86**, 074506 (2012), arXiv:1205.3996 [hep-lat].
[2] A. Alexandru, G. Basar, and P. Bedaque, Phys. Rev. **D93**, 014504 (2016), arXiv:1510.03258 [hep-lat].
[3] H. Fujii, S. Kamata, and Y. Kikukawa, JHEP **11**, 078 (2015), [Erratum: JHEP02,036(2016)], arXiv:1509.08176 [hep-lat].
[4] H. Fujii, S. Kamata, and Y. Kikukawa, JHEP **12**, 125 (2015), arXiv:1509.09141 [hep-lat].
[5] A. Alexandru, G. Basar, P. F. Bedaque, G. W. Ridgway, and N. C. Warrington, (2015), arXiv:1512.08764 [hep-lat].
[6] G. Aarts, Phys. Rev. Lett. **102**, 131601 (2009), arXiv:0810.2089 [hep-lat].
[7] C. Gattringer and T. Kloiber, Nucl.Phys. **B869**, 56 (2013), arXiv:1206.2954 [hep-lat].
[8] C. Gattringer and T. Kloiber, Phys. Lett. **B720**, 210 (2013), arXiv:1212.3770 [hep-lat].
[9] G. Aarts, JHEP **0905**, 052 (2009), arXiv:0902.4686 [hep-lat].
[10] O. Akerlund, P. de Forcrand, A. Georges, and P. Werner, Phys. Rev. **D90**, 065008 (2014), arXiv:1405.6613 [hep-lat].
[11] L. Bongiovanni, K. Langfeld, B. Lucini, R. Pellegrini, and A. Rago, (2016), arXiv:1601.02929 [hep-lat].
[12] M. Cristoforetti, F. Di Renzo, A. Mukherjee, and L. Scorzato, Phys. Rev. **D88**, 051501 (2013), arXiv:1303.7204 [hep-lat].
[13] H. Fujii, D. Honda, M. Kato, Y. Kikukawa, S. Komatsu, and T. Sano, JHEP **10**, 147 (2013), arXiv:1309.4371 [hep-lat].
[14] A. Alexandru, G. Basar, P. F. Bedaque, G. W. Ridgway, and N. C. Warrington, (2016), arXiv:1604.00956 [hep-lat].
[15] V. Vassiliev, *Applied Picard-Lefschetz Theory* (American Mathematical Society, 2002).
[16] J. Milnor, *Morse Theory* (Princeton University Press, Princeton, NJ, 1963).

[17] A. Mukherjee, M. Cristoforetti, and L. Scorzato, Phys. Rev. **D88**, 051502 (2013), arXiv:1308.0233 [physics.comp-ph].

[18] In some singular cases this region can shrink to a line or other manifold with dimension larger than zero but smaller than n. This possibility can be excluded by noticing that, for small $\mathrm{Im}(h)$, the global minimum of S_R on $\mathbb{R}^n$ is very close to ϕ_+, close enough that the quadratic approximation to the action applies. Within the gaussian approximation the flow equations can be solved analytically and the requirement that the region with S_R smaller than $S_R(\phi_+)$ shrinks to a point can be translated on a condition over the "eigenvectors" $\hat{\rho}_i$. We have verified this condition numerically.

[19] J. R. Cash and A. H. Karp, ACM Trans. Math. Softw. **16**, 201 (1990).

[20] A. Alexandru, G. Basar, P. F. Bedaque, S. Vartak, and N. C. Warrington, (2016), arXiv:1605.08040 [hep-lat].